

Hydrodynamic blood plasma separation in microfluidic channels

Maiwenn Kersaudy-Kerhoas · Resham Dhariwal ·
Marc P. Y. Desmulliez · Lionel Jovet

Received: 25 February 2009 / Accepted: 16 April 2009 / Published online: 8 May 2009
© Springer-Verlag 2009

Abstract The separation of red blood cells from plasma flowing in microchannels is possible by biophysical effects such as the Zweifach–Fung bifurcation law. In the present study, daughter channels are placed alongside a main channel such that cells and plasma are collected separately. The device is aimed to be a versatile but yet very simple module producing high-speed and high-efficiency plasma separation. The resulting lab-on-a-chip is manufactured using biocompatible materials. Purity efficiency is measured for mussel and human blood suspensions as different parameters, such as flow rate and geometries of the parent and daughter channels are varied. The issues of blood plasma separation at the microscale are discussed in relation to the different regimes of flow. Results are compared with those obtained by other researchers in the field of micro-separation of blood.

Keywords Reynolds number · Plasma separation · Inertial lift force · Viscous lift force · Bifurcation law

This work was originally presented at the first European conference on Microfluidics, MicroFLU08, December 2008, Bologna, Italy.

M. Kersaudy-Kerhoas (✉) · R. Dhariwal · M. P. Y. Desmulliez
MicroSystems Engineering Centre,
School of Engineering and Physical Sciences,
Heriot-Watt University, Edinburgh EH14 4AS,
Scotland, UK
e-mail: mk87@hw.ac.uk

L. Jovet
Department of Marine Biology, School of Life Sciences,
Heriot-Watt University, Edinburgh EH14 4AS, Scotland, UK

1 Introduction

Blood separation is a strategic preliminary step in the preparation for biological analysis on-chip. Polymerase chain reaction (PCR) can be performed on whole blood but the reaction is inhibited by components of blood such as haemoglobin (cellular portion) and IgG (plasma portion); therefore, by separating blood into its basic components of plasma and cells, the reaction can be optimised for better results (Al-Soud et al. 2000; Al-Soud and Rådström 2001). Moreover, analysis downstream PCR needs clear plasma devoid of cells that would otherwise create interferences if samples were to be analysed optically. Microfluidics permits the analysis of few microliters of biological samples, and avoids painful blood extraction of several dozens of millilitres. Human blood plasma separation has direct, obvious applications in human health monitoring, disease diagnostic and theranostics. Blood plasma separation can however be applied to a variety of other fields, such as environmental pollution monitoring. Indeed, evidence shows that various sea shells and fishes indicate perturbed physiology in polluted areas (Zorita et al. 2007; Zorita et al. 2008). The analysis of toxic compounds such as heavy metals in mussel haemolymph can potentially provide valuable environmental monitoring (Kaloyiannia et al. 2009).

Centrifugation and filtration are the two conventional techniques for blood plasma separation in laboratories. Both methods are time-consuming, relatively expensive and might damage cells if not used carefully (Sallam 1984). In the light of the disadvantages outlined above and the benefits that microscale techniques can provide in terms of volume of blood extracted, response time and portability, it is therefore not surprising that the alternative blood plasma separation on-chip has gained increasing interest

over the last few years. Different types of force available at the microscale have been used to separate blood from plasma on-chip. Such forces are electrical, magnetic and acoustic (Pamme 2007; Kersaudy-Kerhoas et al. 2008). Separation techniques using only hydrodynamic forces, channels geometries and biophysical effects have lately been developed based on preliminary work on microcirculation (Fung 2004). Pharmaceuticals companies like Roche have published reports on the integration possibilities of such preliminary modules (http://www.roche.com/pages/downloads/company/pdf/rddpenzberg02_02e.pdf, last accessed 15 April 2009). A number of studies have been published by different groups. Ducree presented a microlaboratory on a compact disk (CD) that contains a blood plasma separation module (Brenner et al. 2004). This system uses common centrifugal principles. Blatter et al. (2004) proposed a bend structure to increase the plasma-free layer existing naturally in microchannels by using a mini-centrifugal effect. Yang's team presented T-channels to retrieve pure plasma (Yang et al. 2006). Faivre et al. (2006) showed that a constriction integrated in a microchannel increases the cell free-layer up to 1 cm downstream. The addition of spacers near the channels walls allows the pure recollection of plasma. Effenhauser presented a three-dimensional structure taking advantage of a high-aspect ratio to produce a better plasma yield (Jaggi et al. 2007). The plasma yield was defined in this work as the volume percentage of plasma that can be extracted.

The approach chosen in this paper uses the latest advances in hydrodynamic blood plasma separations on-chip. We aim to develop a system with a high plasma yield as well as a low processing time. To allow mass-manufacturability of the device by high volume manufacturing techniques such as microinjection moulding, we used channel dimensions not below 20 μm . The separation method is continuous since no external force field needs to be switched on and off. Moreover the cell and plasma can be continuously collected or directed to in-line processing. The sample injection is kept straightforward and simple, with only one inlet needed for the entire system. In this article, theoretical elements on the design of blood plasma separation system are first explained. A design taking advantage of some biophysical effects such as Zweifach–Fung bifurcation law and axial migration is then presented. In the experimental section, two kinds of biological material have been tested, human blood and mussel blood. Both separations of human blood and mussel blood are quantified and the influence of parameters such as flow rate and configuration of the channels are discussed in relation to the separation efficiency.

2 Design and theoretical discussion


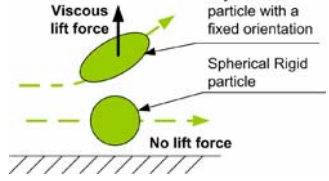


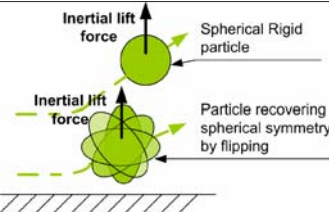
The understanding of the movement of a deformable asymmetric particle, such as a blood cell in a laminar flow, is the key to designing an efficient blood plasma separation microdevice. Although extensive studies of red blood cells (RBCs) behaviour have been carried out over the last 50 years, the prediction of the behaviour of RBCs in a microchannel is a non-trivial problem and some questions still remain unanswered (Abkarian and Viallat 2008). In this section, we will give insights on the fundamental mechanisms occurring in blood plasma separation.

2.1 Red blood cells flow at the microscale

Blood is composed of erythrocytes or red blood cells (RBCs), lymphocytes or white blood cells (WBCs), thrombocytes or platelets, and a plasma used as a carrier fluid. The ratio of WBCs against RBCs is 1: 600–1,000. Blood is known to be a non-Newtonian fluid. However, at the scale close to the microvascular network, blood can be considered as a suspension of RBCs in a Newtonian plasma (Fung 2004). Plasma flow in a microchannel network of hydraulic diameters ranging from 10 to 500 μm is laminar, but the Reynolds number can vary greatly from 0.01 to 100. RBCs are biconcave disks, reported to be extremely deformable. The viscosity ratio between the inner fluid of RBC and the suspending medium partly characterises the behaviour of the RBC in its environment. RBCs are known to exhibit different behaviours and even take different shapes depending on the Reynolds number and the degree of shear force. At a relatively high Reynolds number and viscosity ratio, but in the laminar regime, RBCs flip around themselves; this movement is often referred to as tumbling. At a lower Reynolds number and viscosity, however, the cells follow a tank-treading movement in which the membrane of the cell alone is rotating around the centre of the mass. A cell, which tank-treads, maintains a stationary orientation with the flow (Abkarian and Viallat 2008). Finally, a third transitional regime was found by Abkarian et al. (2007), and is named swinging. In this regime the cell tank-treads but undergoes oscillations around its stationary orientation.

Tank-treading behaviour arises in the absence of inertia. In the presence of a wall, the asymmetry of the flow surrounding the cell leads to a net force creating a drift that pushes the cell to the centre of the channel. Due to this purely viscous lift force, a thin cell-free layer appears on the wall of the channel (Abkarian and Viallat 2008). Faivre et al. (2006) demonstrated that this movement is dependent on the magnitude of the shear force. Thus, the presence of a constriction leads to a local high shear stress zone, pushing

Table 1 This table illustrates the different regimes of cell behaviour in a microchannel of dimensions below 300 μm

Regime and reference	Reynolds number	Viscosity ratio between inner and outer fluids	Movement of cell	Photographic evidence*	Predominant lateral force	Effect in microchannel
A (tank-treading [16])	Very Low (<1)	Low	Tank-treading		Viscous lift force	 <p>Deformable asymmetric particle with a fixed orientation</p> <p>Spherical Rigid particle</p> <p>No lift force</p>
B (Swinging [17])	Low	Medium	Swinging		Transition regime	<i>The different effects on the cells are not known and therefore no drawing can be provided here.</i>
C (Tumbling [16])	Very low to Low (~1)	High	Tumbling		Inertial lift force	 <p>Inertial lift force</p> <p>Spherical Rigid particle</p> <p>Inertial lift force</p> <p>Particle recovering spherical symmetry by flipping</p>

* Photographs of the tank-treading and tumbling cell regimes have been reproduced from reference (Abkarian and Viallat 2008), by permission of the Royal Society of Chemistry. Photograph of the swinging regime has been reproduced from reference (Abkarian et al. 2007) with the authorisation of the authors

the cells even more centrally. Faivre reported a cell-free layer two or three times larger than the one found in the constriction-free channel; such a layer lasts up to 1 cm after the constriction. The lift force is dependent on the shape of particle, deformability of particle, density difference between the particle and the fluid and shear stress. At this regime spherical objects do not experience the lift force, although they have been reported to rotate (Olla 1997).

In this case, an axial migration effect, sometimes referred to as the tubular pinch effect, also applies on spherical and non-spherical particles. The fact that a non-spherical particle rotates fast and thus exhibits the same mechanical characteristics as a spherical particle can explain that non-spherical particles also experience the tubular pinch effect (Olla 1997). The parameters affecting the migration of particles in this regime include the channel diameter-to-particle size ratio, the Reynolds number, the concentration of particles, the shape and deformability of the particle, the density difference between the particle and the fluid, and the presence or absence of particle rotation. In addition, the presence of other forces, such as the Saffman force at relatively high Reynolds number (but still in the laminar

regime), acting on the spherical particles cannot be neglected if the rotation speed of the RBC is high enough.

Some parameters affecting particles movement in a microchannel in the inertial lift or viscous lift are similar although a distinction between these two effects has been theoretically and practically demonstrated in the literature (Abkarian and Viallat 2005). Axial migration is found in the two regimes. In the absence of inertia, deformable asymmetric particles are pulled towards the centre of the channel, while hard spheres do not migrate but follow the streamlines. In the presence of inertia, the opposite scenario is more or less happening, although asymmetric particles have also been observed to move centrally. The frontier between the two regimes has not been clearly established and this adds to the difficulty of predicting the behaviour of specific particles in the microchannels. The three different behavioural regimes: tank-treading, swinging and tumbling, have been classified in Table 1 alongside the conditions required to establish these regimes. The predominant associated force acting laterally relatively to the flow is also given. Photographic evidence from (Abkarian and Viallat 2008) and (Abkarian et al. 2007) is included to illustrate the cell behaviour in the flow. Finally

a schematic summarises the lift effects on rigid and deformable cells for each different regime.

The discussion outlined above concerns the behaviour of cells in straight microchannels. Red blood cells also exhibit a specific behaviour in bifurcations. Fung demonstrated that cells at a bifurcation have a tendency to travel to the highest flow rate daughter channel, providing that the flow rate ratio is at least 2.5:1 and the dimensions of the cells comparable to the channel diameter (Fung 2004). This effect is sometimes referred to as the Zweifach–Fung bifurcation law. Its origin is found in the asymmetrical distribution of pressure and shear forces on the cell at the bifurcation, pulling it to the channel with the highest flow. The effect of the geometry of the bifurcation on the separation has been discussed thoroughly, but opinions still differ. Fung reports that the geometry of the bifurcation enhances the separation mechanism (Fung 2004). If the cell keeps a fixed orientation in the tank-treading regime, then it is easier for the cell to enter into a daughter channel as this one has the same orientation as the cell. Roberts and Olbricht have carried out several experiments on bifurcations to examine whether the angles between the bifurcations are influencing the separation. They demonstrated that the magnitude of the separation depends on the bifurcation geometry and aspect ratio of the channel cross-section (Roberts and Olbricht 2006). On the other hand, Chien et al. (1985) and Pries et al. (1996) reported no appreciable effect of branching angle on the particle distribution at bifurcation. This contradiction illustrates the difficulty of predicting RBCs movement in microchannels. Microfluidic systems can nevertheless take advantage of RBCs specific behaviour to separate plasma from blood.

2.2 Design

The principle of the microfluidic blood plasma separation module is shown in Fig. 1. This design can work at both low and medium Reynolds number which is regulated by the flow rate used (0.01 and 1, respectively). The configuration of the separation module is as follows. First, the use of micrometre dimensions for the microchannel ensures laminar flow and the presence of a particle-free layer. Second, a constriction in the main channel induces a high-shear stress zone pulling the particles even more centrally. Third, 20 bifurcation channels are placed on each side of the main channel to enhance the plasma yield. As the flow rate ratios increase at each bifurcation, the flow rate in the plasma channels might be after a number of bifurcations so low that no plasma will be extracted through these channels. Therefore, it would be unwise to have more than 20 channels without knowing exactly the volumetric flow rate in each plasma channel. In the basic design, the width of the main channel is 100 μm and the plasma channels are

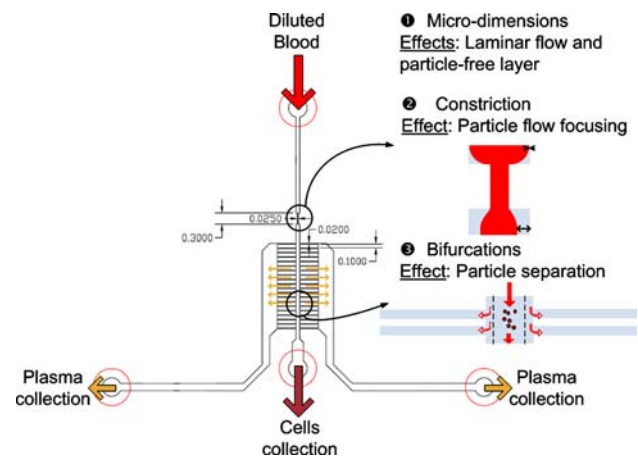


Fig. 1 Principles of the hydrodynamic blood plasma separation. The use of laminar flow ensures a particle free layer on the walls of the main (parent) channel, a constriction pulls the cells even more centrally. Finally, the cells and plasma are separated at the bifurcations using the Zweifach–Fung bifurcation law. Dimensions are given in millimetre

20- μm wide. The constriction width and length are 25 and 300 μm , respectively. These sizes were chosen based on the chip manufacturer specifications (channels have to be larger or equal to 20 μm) and based on the existing literature. The height of all channels is 20 μm . The drift induced on the cells by the constriction has been calculated as (Faivre et al. 2006):

$$d \approx 6\kappa \frac{LR^3}{wh^2} \quad (1)$$

Here L , w , h are the length, width and height of the constriction. R is the radius of a sphere having the same radius as a cell and κ is a dimensionless parameter equal to 0.45. Using Eq. 1 the drift induced by the constriction is estimated to be around 27.5 μm , which means that the cells will be displaced laterally of 27.5 μm after the constriction compared to their lateral position before the constriction. The constriction width and length, and the main channel width have been used as variable parameters and change from one design to another. The external connection consists of only one inlet to introduce the blood and three outlets. One of these outlets collects the cells and the other two collect the plasma. The length of capillaries connected to the outlets can easily be tuned to change the flow rate ratios at the outlets. The length ratio between the plasma outlet capillaries (12 in Fig. 2c) and the cell outlet capillary (11 in Fig. 2c), defined as the *Outlet Length Ratio (OLR)*, has also been used as a variable parameter.

The overall aim of the system is to reach optimum purity efficiency, E_p , defined as:

$$E_p = 1 - \left(\frac{c_p}{c_f} \right) \quad (2)$$

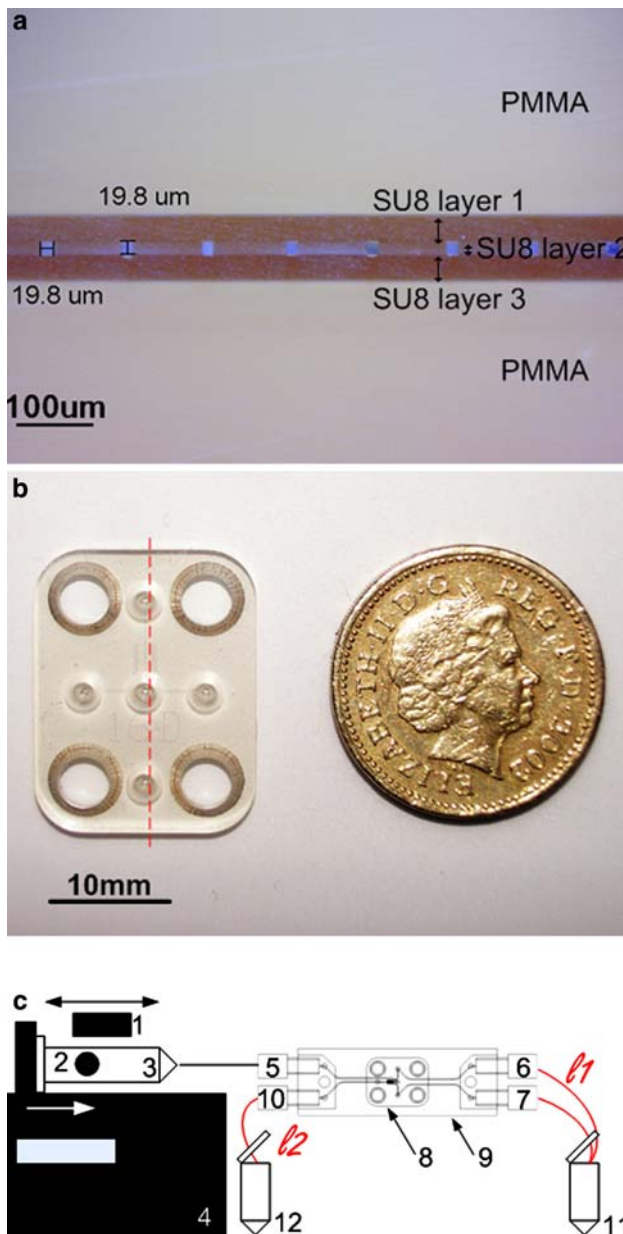


Fig. 2 **a** Cross-section of the plasma channels in the chip. Channels have a blue colour due to previous dyeing. The cross-section measurements and photograph are made using a Dino-Lite microscope and software. **b** Photograph of the chip besides a British pound coin. The red line indicates the cross-section axis of **b**. **c** Diagram of the experimental set-up. 1 magnet, 2 stainless steel ball, 3 syringe, 4 syringe pump, 5 standard tube end fitting at blood inlet, 6 and 7 Standard tube end fittings at plasma outlets, 8 chip (as shown in **b**), 9 fluid adapter component, 10 standard tube end fitting at cell outlet, 11 and 12 Eppendorfs for plasma and cell collection

where c_p and c_f are the number of events per millilitre in the plasma collection outlet and in the feed inlet, respectively. Each event accounts for a particle detected by the flow cytometer used for the analysis. Events can be of biological nature (cells, cell debris or platelets) or of other

nature (dust contaminating the sample). The change of purity efficiency is achieved by varying the following parameters: main channel width, buffer type, outlet length ratio and input flow rate.

3 Experimental set-up

3.1 Prototype manufacture and experimental set-up

Epigem Ltd (Redcar, UK), our industrial partner, has manufactured the chips using a standard lithography process (Epigem Ltd et al. 2009). Chips are made by defining the channel structures photolithographically in SU8 photo resist; 16 individual designs were realised on a standard 6" × 6" substrate size. To make the bonded chip laminates, a PMMA lid layer and base layer were produced. Both PMMA layers were covered with a 30-μm layer of SU8. On top of the 30-μm layer in a further 20 μm thick layer of SU8, were defined the channel features. The additional layers of SU8 ensure that the channels were SU8 on all internal surfaces and additionally enabled the bonding step. The layers stack had the various fluid entry holes drilled into them in registration with the defined channel features. They were then cleaned, layered together in bonding jigs and heated for a time period. The laminate was then divided into separate chips. The different PMMA and SU8 layers forming the chip can be observed in Fig. 2a. A photograph of the fabricated microfluidic chip is shown in Fig. 2b.

Experiments have been carried out on mussel and human blood. Human blood was collected from healthy donors with a sterile lancet (Accu-Check, Roche, Switzerland). The collected blood was suspended in 1 mL of anticoagulant solution composed of Phosphate Buffered Saline (PBS) 1× and 10 μL of ethylene diamine tetraacetic acid trypsin (EDTA-trypsin) (0.05M, Gibco). The immune cells of the blue mussel, *Mytilus edulis*, range from 5 μm up to 25 μm in diameter and were used to investigate the behaviour of larger deformable particles in our system. Additionally, as discussed in the introductory section, mussel blood separation presents an interest for the development of on-site environmental monitoring systems. These immune cells are transparent and have a range of internal complexity. In order to investigate the influence of the buffer type on the purity efficiency, the mussel blood was suspended in two different buffers. The first buffer comprised formaldehyde, known to fix and harden the cells. To keep the cell characteristics as close as possible to the physiological conditions, the second buffer was free of fixing solution. Details of the mussel blood preparation are given in Table 2. A syringe pump was loaded with a 2.5 mL disposable syringe (BD Plastipak). The fluid flow rates used range from 1 to 30 mL/h, although the chip can

Table 2 Table illustrating the preparation of two different buffers for the mussel blood experiments

Buffer preparation	Preparation	Note
With formaldehyde	Five mussels of 4–5 cm in length were bled using 2.5 mL syringe filled with 1 mL of fixing solution (3.6% formaldehyde in 3 × TBS). The haemocyte suspension was centrifuged at 1,000 rpm for 10 min. The cell pellet was re-suspended in 1 mL of methanol and 20 µL of Wright's stain pure solution. After 2 min, 10 mL of TBS buffer was added to the suspension and centrifuged at 1,000 rpm for 10 min. Finally, the cell pellet was re-suspended in 10 mL of fixation solution and ready for use	The cell mixture was kept at room temperature before processing and used in the two hours after bleeding
Without formaldehyde	The mussel blood was collected in a saline solution (v:v) composed of 0.45 M NaCl, 0.1 M glucose, 0.03 M Tris–Sodium citrate, 0.1 M EDTA, 0.026 M citric acid. The pH is adjusted at pH = 8 with KOH	The cell suspensions were kept on ice and used in the following 2 h from extraction

sustain a flow rate of up to 100 mL/h. The chip was connected to a custom-made fluid adapter component (Epigem Ltd) with standard tube end fittings female connectors (Epigem Ltd). The fluidic path from the chip to the fluid adapter is ensured with a Fluence Interconnection System. The overall assembly of the experimental set-up is presented in Fig. 2c. The cellular and plasma sample collection were collected in Eppendorfs via standard 1/16"OD polytetrafluoroethylene (PTFE) tubing connected at the outlets of the assembly system by tube end fittings (Cheminert, VICI Valco Instruments Co. Inc., Houston, TX, USA).

3.2 Measurements

A volume of 200 µL of the sample collections (cell and plasma) was screened using a flow cytometer (FC) (Partec CyFlow SL, Germany). Flow cytometry allows the accurate analysis of cell and particle populations. The flow cytometer focuses individually on the cells in a laminar flow of ultrapure water. The cells pass through a 488 nm blue laser and five characteristics are measured: the relative size of the particles, internal complexity (or granularity), and fluorescence at three different wavelengths (520, 590, and 620 nm). A lower limit has been set up to exclude the particles smaller than 2–3 µm; this filtering allows the reduction of the size of the files stored on the computer. The flow cytometry data was acquired with the Partec FloMax FCM software and analysed with the freeware WinMDI Version 2.9.

4 Results and discussion

In this section experimental results and their analysis are presented to understand the influence of the different parameters on the efficiency of the separation system. The first section concerns the results obtained from the mussel

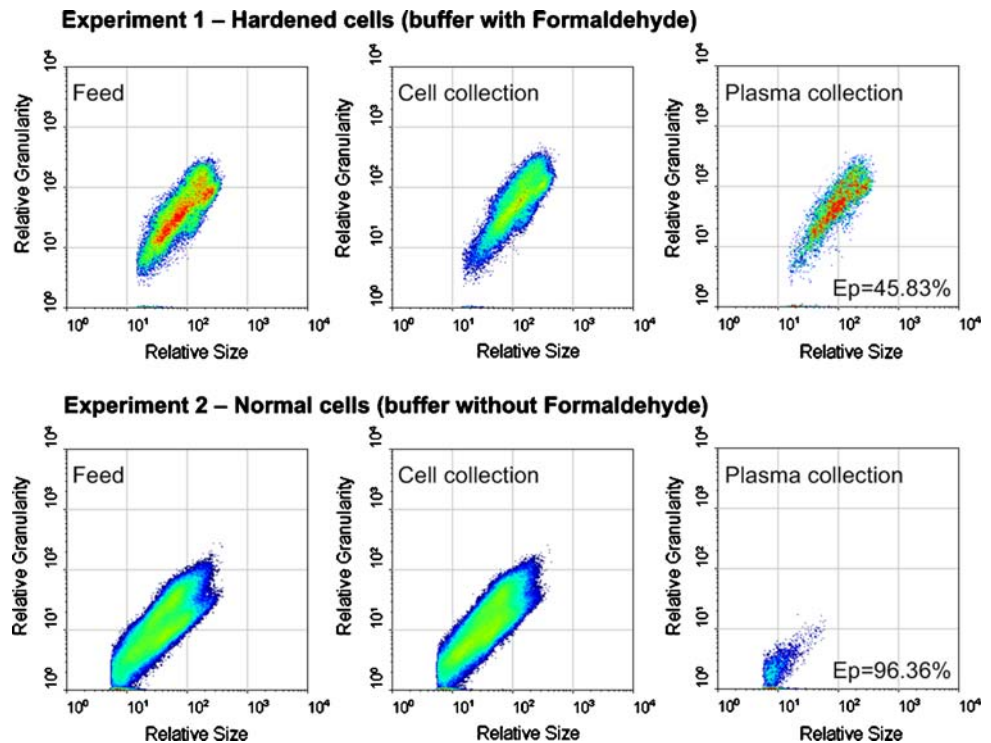
blood separation. The second section presents human blood results. All experiments in this publication have been carried out at large flow rates.

4.1 Mussel blood plasma separation

We were firstly interested in the influence of the buffer type. In Fig. 3, the density plots obtained from the FC results of two experiments are shown. These graphs detail the cell population by displaying the granularity of the cells over their size, in the feed, cell and plasma collection outlets. In both experiments the cell populations have been depleted in the plasma outlet. In both experiments the main channel is 200 µm, the flow rate 10 mL/h, and the Outlet Length Ratio is 3. In Experiment 1, formaldehyde known to harden the cells was used in the mussel cell buffer. The total purity efficiency found was about 46%. In Experiment 2, no formaldehyde or hardening reagent was used in the buffer. The cell population in the plasma collection is largely depleted and the purity efficiency reaches 96%. This result confirms that the cell deformability plays an important role in the separation process.

The influence of the Outlet Length Ratio is also a parameter of interest. In the results presented in Fig. 4, the outlet length ratio varies from 1, 1.8 and 3 in three experiments where the other parameters are kept the same. Figure 4a shows the number of events, particles counted by the FC, when the length ratio is increased threefold, the particle concentration in the plasma collection is still high (70,000 events/mL). To investigate the type of particles present in this population, areas of different cell types (depending on size and granularity) are assigned according to literature on the density plots with WinMDI functions. The percentage of each cell type on the total event count is extracted and compiled into Fig. 4b. In the case of an Outlet Length Ratio of 3, more than 80% of the remaining particles are small particles or cell debris in the order of 3–4 µm.

Fig. 3 Density plot from the flow cytometry results illustrating the influence of the buffer type in two different experiments. In both experiments, the main channel width is 200 μm, flow rate 10 mL/h and Outlet Length ratio, 3. In Experiment 1, the cells are hardened with formaldehyde contained in the buffer solution. In Experiment 2, no hardening solution is used, the cells keep their original deformability. The difference in shape of the cellular fraction is due to the difference in buffer solutions



4.2 Human blood plasma separation

The depletion efficiency of cells in the plasma collection of human blood experiments is generally inferior to the results obtained with mussel blood. This can be partly explained by the difference in cell size. In the human blood the size of the red blood cells ranges from 7 to 8 μm. The cell size is not close to the depth of the channels, and therefore the effect is not as clearly visible as for the larger mussel blood cells.

Figure 5 presents the results of two experiments to determine the influence of the flow rate. These histograms obtained from the FC results show the number of events counted by the FC versus the size of the particle. The Outlet Length Ratio is 4.5 in both experiments, and the flow rate was varied at 5 and 20 mL/h. The results, showing an increase in purity efficiency by 7.6%, suggest that the flow rate might play a role in cell separation.

4.3 Discussion of the results

The results of these experiments have been compared to those published by other groups. The present experiments are undertaken at an average flow rate of 10 ml/h which is significantly higher than previously reported. For reference the average flow rate in publications (Yang et al. 2006; Faivre et al. 2006) is 100 μL/h. Plasma yield is approximately 40%, comparable to Ducrée’s results (Brenner et al. 2004), but it is not reaching the 95% of the common

centrifugation technique. The purity efficiency is calculated as in Eq. 2. The purity efficiency found for the mussel blood is 76.3% on average, with peaks at 96% as shown in Experiment 2, Fig. 3. This last result is comparable to other groups, but has a poor reproducibility. Results of the human blood experiments show a lower efficiency of 53% on average (with a peak at 60.8%), which is below the results reached by other groups. Generally, the hematocrit used in these experiments is low (3%), which means that the blood has to be diluted before the experiments. If the hematocrit was increased, and the experimental conditions were the same, the plasma yield could still reach 40%, but in balance, the purity efficiency would be lower. Table 3 summarises the comparisons made between this publication and other publications in blood plasma separation.

4.4 Discussion about the Reynolds number and the forces acting upon the cells

Although the results of the experiments are satisfactory in terms of purity efficiency as reported earlier, the separation mechanisms happening at the cell level are not as yet fully quantified. In order to gain a better understanding of these mechanisms, it is of interest to present experimental observations of cell flow and compare it with work from other groups. To do so we define the dimensionless channel Reynolds number by μ :

$$R_c = \frac{\rho V D_h}{\mu} \tag{3}$$

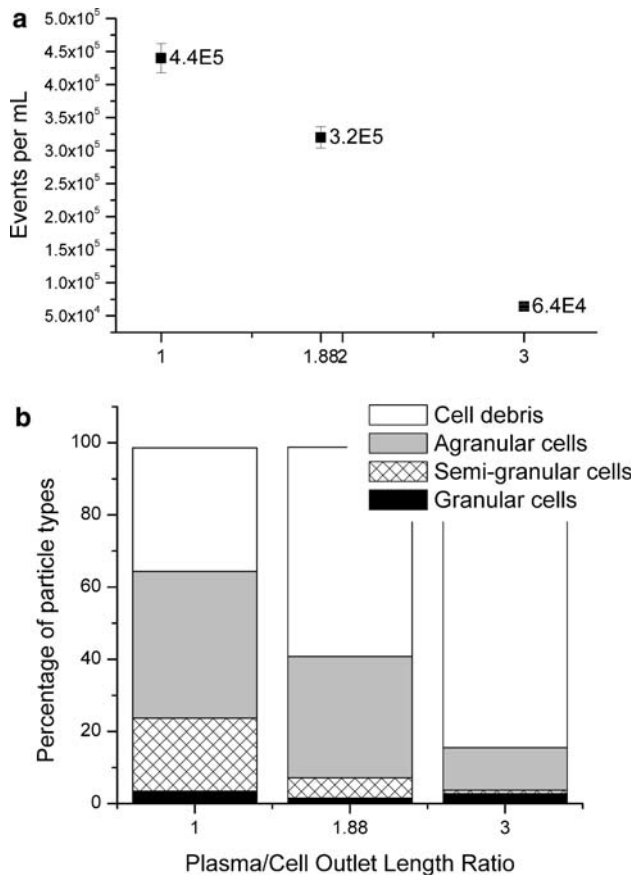


Fig. 4 **a** Graph illustrating the influence of the Outlet Length Ratio on the number of events per mL. **b** Graph illustrating the influence of the Outlet Length Ratio on the repartition of event types in the plasma collection

where ρ is the density of the liquid, μ the viscosity, V the mean velocity across the channel and D_h the hydraulic diameter. Faivre et al. (2006) showed that in their system, rigid spheres did not encounter an axial migration; in other words, the viscous forces overcame the inertial forces. Indeed, the Reynolds number in Faivre was found to be 0.01. In Yang et al. (2006), the Reynolds number is less than 0.01, which also indicates that the system is in the tank-treading regime. However, Jaggi et al. (2007) mention

a higher Reynolds number of up to 5, and yet separation is observed. In these papers, the assumption of a fully laminar regime dominated by viscous forces is made. In our case, for typical flow condition of 10 mL/h the channel Reynolds number was found to be 0.69 (blood viscosity, of 4×10^{-2} Pa s; width, 100 μm ; depth, 20 μm ; density of 10^3 kg m^{-3}). The flow pattern in the system can be easily spotted using a milk mixture. The regime is laminar but recirculating eddies appear after the constriction. Recirculation eddies are not turbulences but secondary laminar flows due to the back-facing step. Although the channel Reynolds number was found to be less than 1, it was observed that the constriction did not focus the cells as much as expected. This can be explained by the fact that the bifurcations create a force on the cells pulling them again towards the main channel walls. In order to compare the behaviour of deformable asymmetric particles with non-deformable spherical ones, we pumped a mixture of 6.6 μm latex spheres in the system and varied the flow rate. Particles were observed when they passed through the constriction using a microscope and videos were recorded. As shown in Fig. 6, at a flow rate of 10 mL/h, the particle-free layer is more important with the latex spheres mixture than with the blood. This proves that the inertial forces are dominating the viscous forces. With flow rates around 200 $\mu\text{L/h}$ or less, the latex beads followed, however, closely the streamlines. At these flow rates the blood cells are expected to focus well; however, we observed only a slight focus much smaller than the 27.5 μm predicted by Eq. 1. The reason for this behaviour might be the effect of the plasma channels placed 500 μm downstream which act on the flow forcing the cells to travel closer to the channel wall.

A further study is necessary to research the transitional behaviour of cells between a fully viscous regime and an inertial regime. Depending on the flow rate used this system has the potential to achieve two modes of separation. One mode would separate hard spheres using the inertial lift force; while the other one would separate soft deformable particles using a viscous lift force. Consequently, the use of a lower flow rate for the full viscous mode would significantly reduce the plasma yield.

Fig. 5 Figure illustrating the influence of the flow rate on the purity efficiency in the human blood experiments. The black peak on the first graph is an artifact

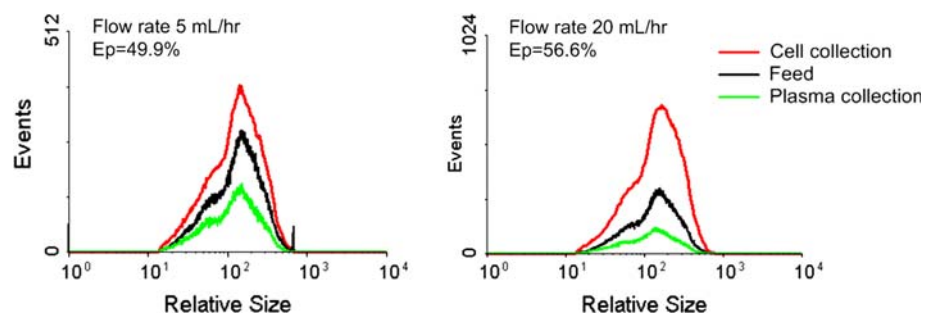


Table 3 Table illustrating the comparison between different blood plasma separation microtechniques and the common centrifugation process

	Brenner et al. (2004)	Faivre et al. (2006)	Jaggi et al. (2007)	Blattert et al. (2004)	Yang et al. (2006)	Common centrifugation	This work
Flow rate (mL/min)	15×10^{-3}	3.3×10^{-3}	5	1.2	1.67×10^{-3}	Batch	0.167
Hematocrit (%)	45	16	4.5	5	<25	45	3
Counting method	Optical (colour recognition)	NC	Auto cell counter	Auto cell counter	Optical (image analysis)	FC	FC
Regime used (refer to Table 1)	Centrifugation on a CD	A	C	Small centrifugal force + C (predominant)	A	Centrifugal force	C (10 mL/h)
Plasma yield (%)	40	18	2.5	3	19	95	40
Purity efficiency (%)	99	100	90	90	100	99	76.3% Mussel Blood (with peaks at 96%) 53% Human Blood

The behaviour of the RBCs is also indicated with reference to Table 1

NC non-communicated, FC flow cytometry

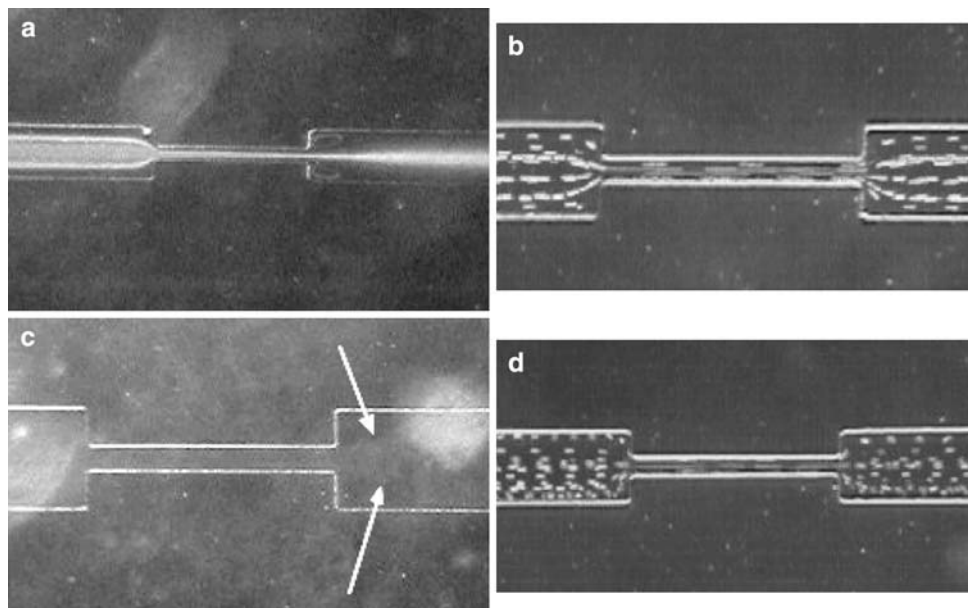


Fig. 6 **a** A photograph of 6.6 μm latex spheres passing through the constriction ($25 \times 300 \mu\text{m}$). The flow rate is 20 mL/h. The flow is from left to right in all photographs. The focus is clearly visible at the end of the constriction (**b**). A stack of photographs of 6.6 μm latex beads at a flow rate of 5 $\mu\text{L/h}$. Each sphere is following a flow streamline. **c** A photograph of red blood cells passing at 20 mL/h in

the constriction. The focus is less accentuated than in **a** and the cells retrieve their position near the walls only 150 μm after the constriction. Two *white arrows* are pointing onto the focused cell stream. **d** A stack of photographs of red blood cells passing through the constriction at a flow rate of 5 $\mu\text{L/h}$. Here a focus of a few microns is visible after the constriction

5 Conclusions

This article presents a new arrangement of channels for blood plasma separation. It has been demonstrated that cells can be separated from plasma at high flow rate using biophysical effects. This technique allows the integration of downstream analysis modules, and therefore can be considered fully continuous. The chip has been manufactured

with low-cost biocompatible material. The conventional photolithographic technique can be applied to small scale (prototyping) and large scale (production) without increase in costs or manufacturing time. According to the material and the geometries needed, this technique can be replaced by even cheaper techniques such as microinjection moulding allowing thereby low-cost mass-manufacturing. Experimental results show that the separation efficiencies

obtained are in good agreement with previous studies, but provide a better plasma yield. A study on the viability of cells after separation has been omitted from this work, and, although the cells seem to support well the process, further studies need to be undertaken in that regard. The issues of blood plasma separation on-chip have been discussed. This study suggests that more detailed research should be carried out on the transitional regime in which inertial and viscous forces are balanced.

Acknowledgments The authors acknowledge the financial support of the Engineering and Physical Science Research Council (EPSRC) through the funding of the Grand Challenge Project ‘3D-Mintegration’, reference EP/C534212/1. We thank Tim Ryan and Phil Summersgill, Epigem Ltd. for the fabrication of the chips. The fabrication work was carried out in the Fluence Microfluidics Application Centre supported by the Technology Strategy Board (TSB) and the OneNE Regional Development Agency as part of the UK’s MNT Network. The authors thank Deirdre Kavanagh for careful reading of the manuscript.

References

- Abkarian M, Viallat A (2005) Dynamics of vesicles in a wall-bounded shear flow. *Biophys J* 89(2):1055–1066
- Abkarian M, Viallat A (2008) Vesicles and red blood cells in shear flow. *Soft Matter* 4:653–657
- Abkarian M, Faivre M, Viallat A (2007) Swinging of red blood cells under shear flow. *Phys Rev Lett* 98(18):188302
- Al-Soud WA, Rådström P (2001) Purification and characterization of PCR-inhibitory components in blood cells. *J Clin Microbiol* 39:485–493
- Al-Soud WA, Jönsson LJ, Rådström P (2000) Identification and characterization of immunoglobulin G in blood as a major inhibitor of diagnostic PCR. *J Clin Microbiol* 38:345–350
- Blattert C, Jurischka R, Tahhan I, Schoth A, Kerth P, Menz W (2004) Separation of blood cells and plasma in microchannel bend structures. In: Proceedings of eighth international conference on miniaturized systems for chemistry and life sciences, pp 483–485
- Brenner T, Haerberle S, Zengerle R, Ducree J (2004). Continuous centrifugal separation of whole blood on a disk. In: Proceedings of eighth international conference on miniaturized systems for chemistry and life sciences, pp 566–568
- Chien S, Tvetenstrand CD, Epstein MAF, Schmidtschonbein GW (1985) *Am J Physiol* 248:H568–H576
- Epigem Ltd, www.epigem.co.uk, last accessed 19 April 2009
- Faivre M, Abkarian M, Bickraj K, Howard S (2006) Geometrical focusing of cells in a microfluidic device: an approach to separate blood plasma. *Biorheology* 43:147–159
- Fung YC (2004) *Biomechanics*, 2nd edn. Springer, New York
- Jaggi RD, Sandoz R, Effenhauser CS (2007) Microfluidic depletion of red blood cells from whole blood in high-aspect-ratio microchannels. *Micro NanoFluid* 3:47–53
- Kaloyiannia M, Dailianisa MS, Chrisikopoulou E, Zannoua A, Koutsogiannakia S, Alamdarib DH, Koliakosb G, Dimitriadis VK (2009) Oxidative effects of inorganic and organic contaminants on haemolymph of mussels. *Comp Biochem Physiol C* (in press)
- Kersaudy-Kerhoas M, Dhariwal RS, Desmulliez MPY (2008) Recent advances in microparticle continuous separation. *IET Nanotechnol* 1:1–13
- Olla P (1997) The lift on a tank-treading ellipsoidal cell in a shear flow. *J Phys II* 7(10):1533–1540
- Pamme N (2007) Continuous flow separations in microfluidic devices. *Lab Chip* 7:1644–1659
- Pries AR, Secomb TW, Gaehtgens P (1996) Biophysical aspects of blood flow in the microvasculature. *Cardiovasc Res* 32:654–667
- Roberts BW, Olbricht WL (2006) The distribution of freely suspended particles at microfluidic bifurcations. *AIChE J* 52:199–206
- Sallam AM (1984) Human red blood-cell hemolysis in a turbulent shear-flow—contribution of Reynolds shear stresses. *Biorheology* 21:783–797
- Yang S, Undar A, Zahn JD (2006) A Microfluidic device for continuous, real time blood plasma separation. *Lab Chip* 6:871–880
- Zorita I, Apraiz I, Ortiz-Zarragoitia M, Orbea A, Cancio I, Soto M, Marigomez I, Cajaraville MP (2007) Assessment of biological effects of environmental pollution along the NW Mediterranean Sea using mussels as sentinel organisms. *Environ Pollut* 148:236–250
- Zorita I, Ortiz-Zarragoitia M, Apraiza I, Cancio I, Orbea A, Soto M, Marigómez I, Cajaraville MP (2008) Assessment of biological effects of environmental pollution along the NW Mediterranean Sea using red mullets as sentinel organisms. *Environ Pollut* 153(1):157–168